International Journal of Nanomedicine

Dovepress
open access to scientific and medical research

Open Access Full Text Article

ORIGINAL RESEARCH

Anti-CD30-targeted gold nanoparticles for photothermal therapy of L-428 Hodgkin's cell

This article was published in the following Dove Press journal:
International Journal of Nanomedicine
13 December 2012
Number of times this article has been viewed

Xiaochao Qu[1,2,*]
Cuiping Yao[2,*]
Jing Wang[2]
Zheng Li[2]
Zhenxi Zhang[2]

[1]Life Sciences Research Center, School of Life Sciences and Technology, Xidian University, Xi'an, Shaanxi, China; [2]Key Laboratory of Biomedical Information Engineering of Education Ministry, Institute of Biomedical Analytical Technology and Instrumentation, School of Life Science and Technology, Xi'an Jiaotong University, Xi'an, Shaanxi, China

*These authors contributed equally to this work

Purpose: Due to the efficient bioconjugation and highly photothermal effect, gold nanoparticles can stain receptor-overexpressing cancer cells through specific targeting of ligands to receptors, strongly absorb specific light and efficiently convert it into heat based on the property of surface plasmon resonance, and then induce the localized protein denaturation and cell death.

Methods: Two gold nanoparticle–antibody conjugates, gold-BerH2 antibody (anti-CD30 receptor) and gold-ACT1 antibody (anti-CD25-receptor), were synthesized. Gold-BerH2 conjugates can specifically bind to the surface of L-428 Hodgkin's cells, and gold-ACT1 conjugates were used for the control. The gold nanoparticle-induced L-428 cell-killing experiments were implemented with different experimental parameters.

Results: At a relatively low concentration of gold and short incubation time, the influence of cytotoxicity of gold on cell viability can be overlooked. Under laser irradiation at suitable power, the high killing efficiency of gold-targeted L-428 cells was achieved, but little damage was done to nontargeted cancer cells.

Conclusion: Gold nanoparticle-mediated photothermal therapy provides a relatively safe therapeutic technique for cancer treatment.

Keywords: gold nanoparticle–antibody conjugates, surface plasmon resonance, laser irradiation, selective destruction, photothermal treatment, cancer

Introduction

Cancer is a significant cause of morbidity and mortality in patients. More than 10 million patients with new cases of cancer are diagnosed every year, and about 27 million new cases of cancer will have been recorded by 2030.[1,2] Some traditional cancer therapies, such as radiotherapy and chemotherapy, have enhanced the 5-year survival rates of cancer patients. For improving the therapeutic efficiency against cancer, increasing amounts have been used to develop more new approaches, with the aims of fewer side effects, enhanced safety, and decreased invasiveness.

Hyperthermia is known to induce apoptotic cell death in many tissues, in which the local temperature is raised more than 40°C. The heat generation sources, radiofrequency waves, microwaves, or ultrasound, have been used to produce moderate heating in a specific target region.[3] Heat energy can cause irreversible cell damage by denaturing proteins and the local cells or tissues are selectively destroyed. Thus, hyperthermia is more sensitive to the effects of conventional therapeutic strategies. However, a lack of specificity for tumor tissues would induce unavoidable cell damage in the surrounding healthy tissues, which has limited use in cancer treatment.[3] While still in a relatively

Correspondence: Zhenxi Zhang
Institute of Biomedical Analytical Technology and Instrumentation, School of Life Science and Technology, Xi'an Jiaotong University, Nr 28 Xianning Xi Road, Xi'an 710049, People's Republic of China
Tel/fax +86 29 8266 6854
Email zxzhang@mail.xjtu.edu.cn

Xiaochao Qu
Life Sciences Research Center, School of Life Sciences and Technology, Xidian University, 2 South Taibai Road, Xi'an, Shaanxi 710071, People's Republic of China
Tel +86 29 8189 1070
Fax +86 29 8189 1060
Email xiaochaoqu@gmail.com

immature stage, gold nanoparticle-mediated photothermal therapy has contributed to great advances in cancer therapy.

Gold nanostructures, as highly biocompatible materials, are widely used for biological application and medical purposes including imaging, drug delivery, and hyperthermia therapy.[4–6] Gold nanostructures provide precise control of sizes, shapes, and flexible surface chemistry for bioconjugation of biological molecules, which can offer molecular-level specificity for particular biocoupling in cancer cells. Due to unique and highly tunable optical properties, when gold nanostructures are exposed to light at their resonance wavelength, the conduction band electrons at the gold surface generate a collective coherent oscillation, resulting in strong light absorption or light scattering of gold. The absorbed light can be converted into localized heat, which can be readily employed for therapy based on photothermal destruction of cancer cells.[7–10] Pitsillides et al first reported the photothermal therapy in lymphocytes with a short pulsed laser in the presence of gold nanoparticle immunoconjugates in 2003.[11] Zharov et al reported gold-induced thermal destruction of cancer cells using a nanosecond laser.[12,13] Research on the use of gold in cancer treatment has also been carried out by El-Sayed et al.[10,14] Several studies have reported on the feasibility and efficiency of tumor-specific targeting of gold nanostructures for photothermal cancer therapy, such as gold nanorods,[15] nanoshells,[5,16] and nanocages.[17]

In this study, on the basis of successfully synthesizing gold nanoparticle-antibody conjugates, L-428 Hodgkin's cell-killing experiments induced by the photothermal effect of gold nanoparticles were implemented. Under laser irradiation, through specific targeting of ligands to receptors, light strongly absorbed by gold is transferred to the antibody molecules and the cell environment, so that the very high killing efficiency of cancer cells can be achieved.

Materials and methods

Photothermal therapy system

The photothermal therapy experimental setup is shown schematically in Figure 1. The irradiation laser was a frequency doubled Q-switched neodymium (Nd):YAG laser (Surelite I; Continuum, Santa Clara, CA), with nonlinear crystals to enable conversion of the fundamental wavelength frequency from 1064 nm to 532 nm (2.5 mm spot size, 6 ns pulse width, 10 Hz repetition rate), which was used for matching the gold surface plasmon resonance peak for photothermal cancer treatment. The output laser power, which is measured with a power meter, was adjusted by using an attenuator placed between the laser and the first mirror. Then, the laser was irradiated on a sample micro-cuvette with 18 wells with a diameter of 2 mm, which was custom-made in a 25 × 75 mm optical glass slide.

Synthesis of gold nanoparticle-antibody conjugates

The two antibodies, anti-CD30 monoclonal antibody (mAb) BerH2 and anti-CD25 mAb ACT1, were provided by the Research Center Borstel (Borstel, Germany). Gold nanoparticles 15 nm in size were purchased from British Biocell International Ltd (Cardiff, UK). The stable gold–antibody conjugates were prepared by passive absorption of proteins to the surface of the gold. For steady conjugation of antibodies and gold, the pH of the gold solution must be adjusted to be just above (~0.5) the isoelectric point (pI) of the antibody.[18] An important parameter to consider is the amount of antibody bound to the gold.

To find the amount of antibody needed to saturate and stabilize the gold, a titration procedure was used to fix the antibody concentration using a 96-well microtiter plate. First, 50 µL solution with the same concentration of gold per well was placed into ten plates. The pI of BerH2 and ACT1 antibodies was about 7.5, the pH of the gold in every plate was adjusted by 1% K_2CO_3 solution to 8.0 to match the pI of the protein. Then, various amounts of antibodies with the same concentration were added. After stewing for 5 minutes, 10 µL of NaCl solution (10%) per well was added and mixed homogenously, while observing the solution color change. The amount that maintained the red color before the blue envelope was used for conjugation. For gold-BerH2 and gold-ACT1 conjugates, 70 µL 1% K_2CO_3 solution was added into 5 mL gold to make the pH = 8.0, and the best conjugation amount of BerH2 (9.5 mg/mL) was 7.5 µL, while the best conjugation amount of ACT1 (7.4 mg/mL) was 12.5 µL.

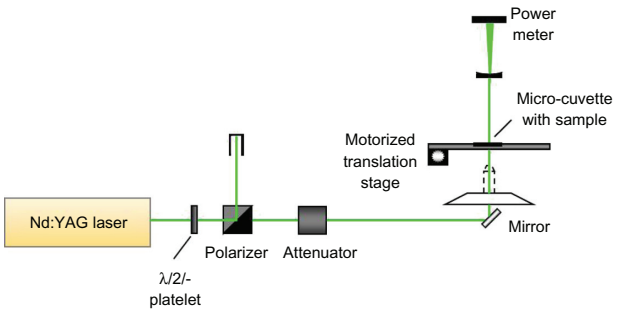

Figure 1 Schematic diagram of the Nd:YAG laser irradiation system.
Abbreviation: ND, neodymium.

To take the preparation of gold-BerH2 conjugates as an example, 5 mL gold nanoparticles with 15 nm were transferred into a 15 mL tube, and 70 µL 1% K_2CO_3 solution was added into the tube to adjust the pH. Then, 7.5 µL BerH2 mAbs (9.5 mg/mL) were mixed into the gold solution. After incubating for 30 minutes at room temperature while stirring, the solution was centrifuged for 30 minutes at 13,000 rpm. The bottom scarlet solution was extracted and centrifuged for 45 minutes at 40,000 rpm to wash the unbound antibodies. Finally, the pellet was resuspended in phosphate-buffered saline (PBS) supplemented with 0.1% bovine serum albumin (BSA), and stored at 4°C until use.

Cell culture and sample preparation

The L-428 human lymphoma cell line was provided by the Research Center Borstel. Cells were maintained in RPMI1640 medium supplemented with 10% heat-inactivated fetal calf serum, 2 mM L-glutamine, and antibacterial antibiotic solution. The cell line was maintained at 37°C in an incubator in 5% CO_2 and 95% air and passaged twice a week. For the experiments, L-428 cells at the logarithmic growth phase were centrifuged at 1400 rpm for 5 minutes at 20°C and then resuspended in PBS with cell densities of 10^6 mL^{-1}.

For testing the stability of gold–antibody conjugates and the staining ability of different conjugates to the L-428 cells, either gold-BerH2 or gold-ACT1 conjugates were added to the cell suspension at certain ratios between the conjugates and the cells. After incubation for 20 minutes at 37°C, the cells were centrifuged and washed twice and resuspended in PBS. Then, a secondary antibody, goat anti-mouse Alexa 488 (aM-A488) was added into the cell suspension to couple with the BerH2 or ACT1 antibody. After incubation for 20 minutes and centrifugation at 1400 rpm for 5 minutes, the cell samples were resuspended in PBS and analyzed using a flow cytometer (FACScan; Becton Dickinson, Franklin Lakes, NJ). Equipped with a 488 nm air-cooled argon-ion laser. Data analysis was based on the collection of 10,000–50,000 events.

To implement the gold nanoparticle-induced L-428 cell-killing experiments, the gold–antibody conjugates, gold-BerH2 and gold-ACT1, and unbound gold with the same optical density, were added into the cell suspension, respectively. After incubation for 20 minutes at 37°C, the cells were centrifuged at 1400 rpm for 5 minutes, and resuspended in PBS for the next photothermal treatment.

Photothermal treatment

In the L428 cell killing experiments, there were four experimental groups for comparing the killing efficiency with or without gold, the control cell group, cells with unbound gold, cells with gold-BerH2 conjugates, and cells with gold-ACT1 conjugates. Four groups of prepared cell samples was seeded into sample micro-cuvettes per well. The cells were treated in the scanning mode of laser irradiation with 0–50 mW, 5 pulses. After photothermal treatment, all of the cells were washed, resuspended in PBS, and incubated for 15 minutes, followed by the cell viability analysis.

Cell viability analysis

Cell viability was determined using calcein-AM/propidium iodide (PI) double-staining solution. Briefly, after photothermal treatment, 2 µg/mL of calcein-AM solution was added into the irradiated resuspended cell sample and incubated at 37°C for 20 minutes. Then, 1 µg/mL of PI was added. The samples were analyzed using flow cytometry. To determine the percentage of necrotic cells relative to the total number of cells, 10,000–50,000 events were acquired per sample using CELLQuest software (BD Biosciences). All the data were processed with WinMDI 2.8 software (Microsoft Corporation, Redmond, WA). Samples were run in triplicate. The results were confirmed by fluorescence microscopy (BH2-RFL-T2; Olympus Corporation, Tokyo, Japan), and the fluorescent images were recorded using a digital camera.

Results

Cell-binding specificity of gold nanoparticle–antibody conjugates

To evaluate the conjugation stability of gold and antibodies and the binding specificity of different conjugates to L-428 cells, the two conjugates, gold-BerH2 (anti-CD30 receptor) and gold-ACT1(anti-CD25 receptor), and the goat anti-mouse Alexa 488 were adopted in this experiment. Both CD30 and CD25 are cell membrane proteins of the tumor necrosis factor receptors, but only CD30 has a high overexpression on the surface of L-428. Through the specific coupling of goat anti-mouse immunoglobulin G antibody to monoclonal antibody, stable coupling was achieved between aM-A488 and BerH2/ACT1. Whether or not aM-A488 attaches to L-428 depends on the expression of protein on L-428. Flow cytometry measurements are shown in Figure 2. About 50,000 events were acquired per sample. The results indicate that only for the cells in the gold-BerH2 group, the detection of the fluorescence

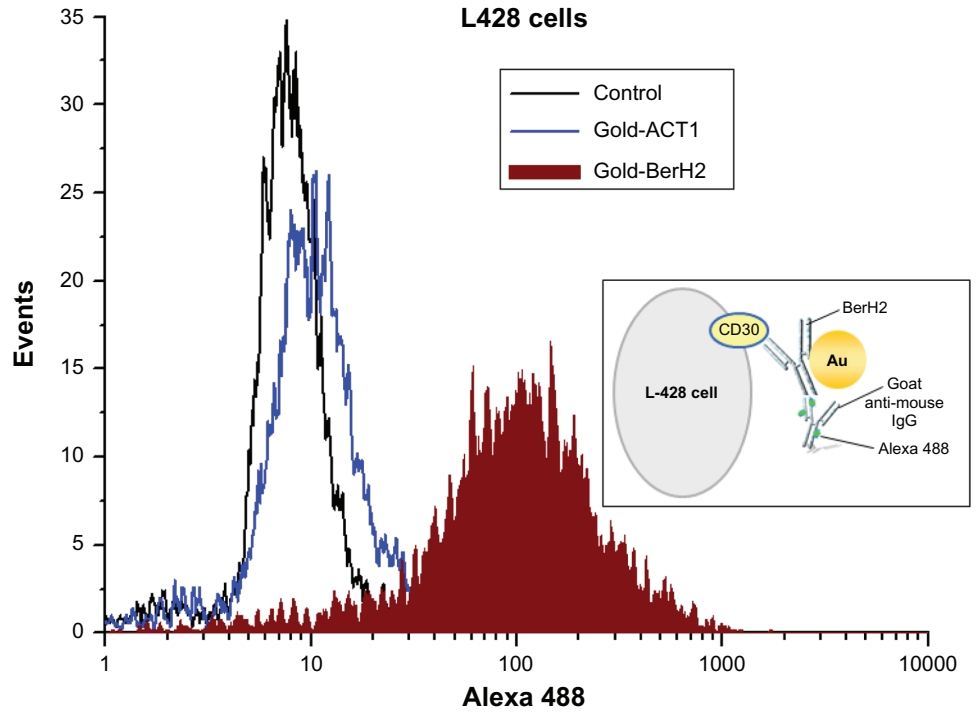

Figure 2 Flow cytometry detection of the binding specificity of different gold nanoparticle–antibody conjugates.
Note: The inset box shows the conceptual diagram of L-428 cells stained with gold-BerH2 conjugates and aM-A488.
Abbreviation: Ig, immunoglobulin.

signal was positive. The fluorescence signal on the cells in the gold-ACT1 group was the same as that for the control cell group (negative). L-428 was positive for CD30, but negative for CD25. As a result, the gold-BerH2 conjugates bound specifically to CD30 receptors on the surface of L428 cells, which were also stained with aM-A488. A conceptual diagram of this binding process is shown in the inset box in Figure 2. The conjugation stability was confirmed on one hand, but the different binding abilities of different conjugate-bound cells would bring a different performance in the cell-killing experiment.

Cytotoxicity of gold nanoparticles

Figure 3 shows cell viability of L428 cells after some hours of exposure to a certain concentration of gold, or gold-BerH2 conjugates. The ratio of pure gold to cells was 10^4:1, and the ratios of gold conjugates to cells were 10^4:1 and 10^8:1, respectively. The concentration of conjugates was increased to determine gold's potential cellular toxicity. After incubation, the number of viable cells were stained with calcein-AM (2 μg/mL) and then measured using flow cytometry. For all samples, 20,000 events were acquired.

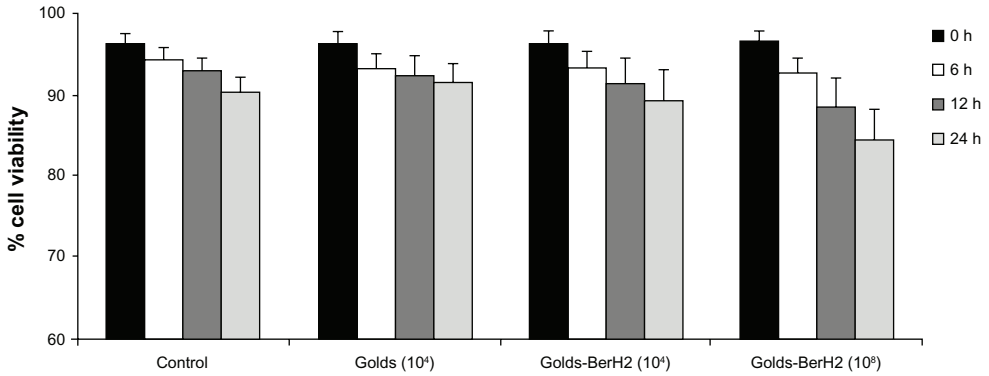

Figure 3 Viability of L-428 cells exposed to either unbound golds or gold-BerH2 conjugates for 6, 12, and 24 hours, as evaluated by flow cytometry.
Notes: Percentage was calculated as the ratio of calcein-AM uptake with L-428 cells divided by the total cells, as calculated for each condition. Control: L-428 cells without gold. Gold (10^4): L-428 incubated with unbound gold at the ratio of 10^4:1. Gold-BerH2 (10^4) and Gold-BerH2 (10^8): L-428 incubated with gold-BerH2 conjugates at the ratios of 10^4:1 and 10^8:1. Error bars represent 1 standard deviation.

For the groups of unbounded gold and gold-BerH2 conjugates incubated with L-428 cells at a ratio of 10^4, the cell viability was greater than 90% after 24 hours of incubation, which had no significant difference compared with the control cell group. At the ratio of 10^8:1, a bigger decrease in cell viability was observed after incubation for 24 hours and L-428 cell viability dropped to 84%. Therefore, for a short incubation period (less than 12 hours), there was no significant increase in the number of dead cells incubated with gold at a relatively low concentration. To avoid the cytotoxicity induced by gold with high doses and a long incubation period, the highest ratio of gold to cells used for the photothermal killing experiment was not more than 10^4:1, and the incubation period was less than 6 hours.

The effect of laser-irradiated power in cell viability in the presence of gold–antibody conjugates

To monitor the necrotic effect of laser irradiation on living cells in the presence of gold, we performed cell damage experiments on L-428 cells, which were incubated with gold-BerH2 conjugates at a 10^4:1 ratio for 20 minutes, and then irradiated with a laser at 50 mW, 5 pulses. After irradiation, cell viability was assessed using calcein-AM (2 µg/mL) and PI (1 µg/mL) staining, and tested using flow cytometry and optical fluorescence microscopy. The events for FACS were 20,000 events. The living cells were stained positively with calcein-AM solution. The cells positively stained with PI presumably represented the later stages of cell death, when membrane integrity was lost. The percentage of death was calculated as the number of PI positive cells divided by the total number of cells.

Figure 4 shows the photothermal treatment results, where severe destruction of L-428 cells was observed when the cells were exposed to laser irradiation (50 mW, 5 pulses) with gold-BerH2 conjugates. The flow cytometry results of L-428 cells incubated with gold-BerH2 conjugates treated with or without laser irradiation are shown on the left side. The corresponding fluorescent images are shown on the right side. Without laser irradiation, about 93% of the cell population was alive, which exhibited bright green fluorescence after calcein-AM staining. More than 95% of the cell population was dead after laser irradiation at 50 mW, 5 pulses, and the dead targets exhibited red fluorescence after PI staining.

Furthermore, the effect of laser influence on laser-induced cell damage has been considered in this section. To test whether the increased cell death rate is linked to laser irradiated power, we treated cell samples with different laser power settings. L-428 cells incubated

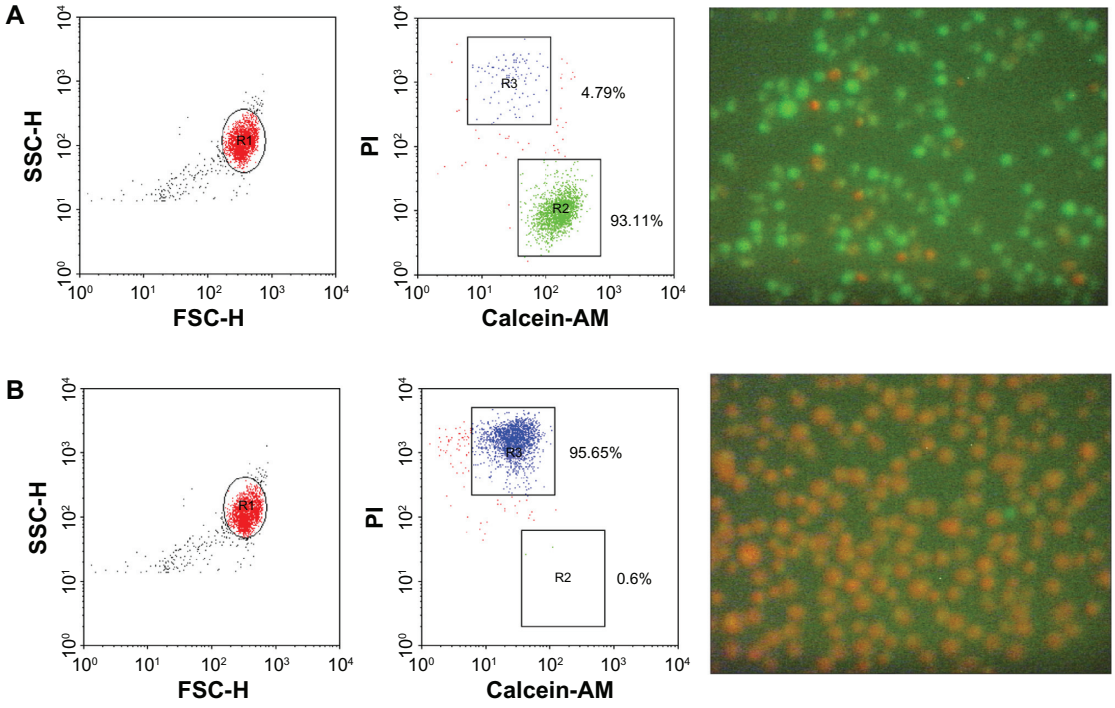

Figure 4 Photothermal treatments of L-428 cells with gold-BerH2 conjugates. (**A**) With 532 nm laser irradiation with 50 mW, 5 pulses; (**B**) without laser irradiation.
Notes: Cells were stained using calcein-AM and propidium iodide solution, and then analyzed using flow cytometry and a fluorescence microscope. The left side of the figure shows dot plots. The fluorescent images on the right side show calcein-AM (green).
Abbreviations: FSC-H, forward light scatter-height; PI, propidium iodide; SSC-H, side light scatter-height.

with gold-BerH2 conjugates and the control cell group were seeded into the sample micro-cuvette respectively. The cell concentration was 4×10^6/mL, and the gold-BerH2 conjugate to cell ratio was 10^4:1. The cell samples were irradiated with 5 pulses and different laser power settings, and then tested using the flow cytometry by calcein-AM/PI double staining. Figure 5A and B show a representative flow cytometry dot plot illustrating the change in cell viability induced by different power laser irradiation. Right lower quadrants expressed the calcein-AM positive cells as a percentage of the total cell population. Left upper quadrants expressed the PI positive cells as a percentage of the total cell population. As shown in Figure 5A, for the control cell group, there was no remarkable change in cell viability when increasing the laser-irradiated power from 0 mW to 50 mW. But for the cells in the gold-BerH2 conjugates group as shown in Figure 5B, cell damage efficiency was affected significantly by the laser-irradiated power. The cell death rate was about 40% when using 15 mW laser irradiation; most of the cells died when the laser power was increased to 50 mW. In the presence of gold–antibody conjugates, the cell death rate mostly depends on the laser irradiated power.

The statistical analysis of the repeated experiments is shown in Figure 5C. For the control cell group incubated without gold, the cell viability curve did not change much with the variation of laser-irradiated power; however, the curve of the cells with gold-BerH2 conjugates showed a rapid decrease in cell viability as the laser power increased. Excessive irradiated laser power caused devastating damage or complete necrosis of L-428 cells incubated with gold–antibody conjugates. Due to the specific aggregation of the CD30 receptor and BerH2 antibodies, gold-BerH2 conjugates were bound tightly to the surface of L-428 cells. Efficient conversion of light strongly absorbed by the gold to heat energy induced a significant increase in cell death.

Cell viability induced by different binding modes of gold to cells

The effect of the photothermal treatment of L-428 cells was evaluated in the above experiments by combining laser irradiation and gold nanoparticles. In this section, we compared the efficiency of different binding modes of gold to cells and cell viability. There were four experimental groups for comparing the killing efficiency with or without gold nanoparticles: the control cell group, cells with gold, cells with gold-BerH2 conjugates, and cells with gold-ACT1 conjugates. From the cell-binding specificity tests, it was known that BerH2 antibodies could bind specifically on the surface of L-428 cells, but ACT1 antibodies could not. Thus, the above four experimental groups represented four combination conditions between gold and cells: pure cells, cells with unbound gold, cells targeted by few nonspecific gold–antibody conjugates, and cells targeted by many specific gold–antibody conjugates. The cell samples were treated by laser irradiation with 40 mW, 5 pulses, which would be compared with the nonirradiated part. Then, 10,000 events were tested using flow cytometry by calcein-AM/PI double-staining.

The experimental analysis results are shown in Figure 6, and were divided into two parts: irradiated and non-irradiated. In the non-irradiated part, there was no difference of

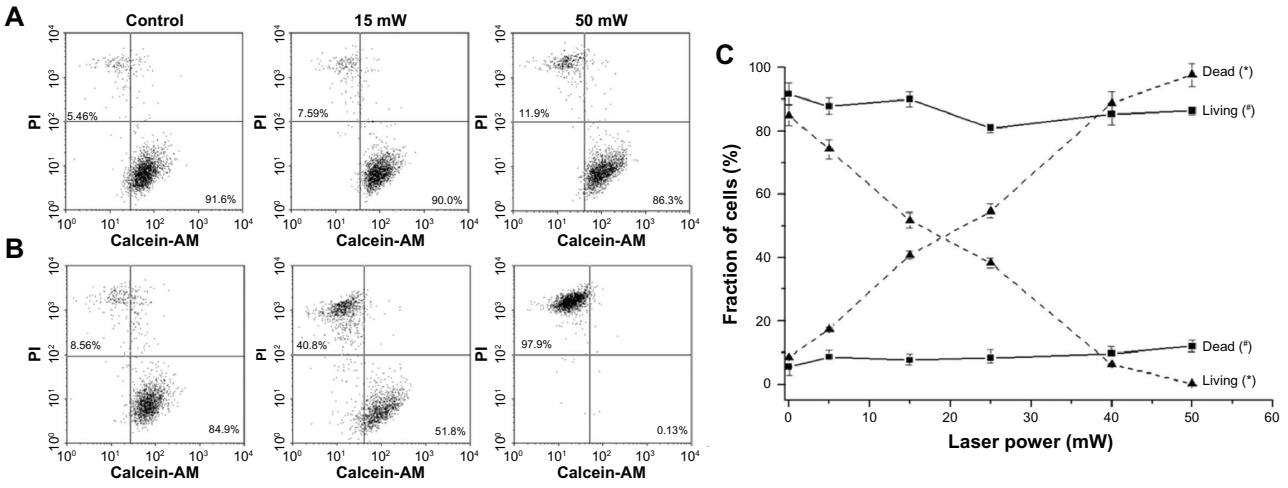

Figure 5 Flow cytometry dot plot and statistical analysis diagram of L-428 cells after being irradiated at different laser power settings. (**A**) L-428 cells; (**B**) L-428 cells incubated with gold-BerH2 conjugates. (**C**) The results were analyzed by flow cytometry data.
Notes: *L-428 incubated with gold-BerH2 conjugates; #L-428 incubated without gold-BerH2 conjugates. Error bars represent 1 standard deviation.
Abbreviations: mW, microwatts; PI, propidium iodide.

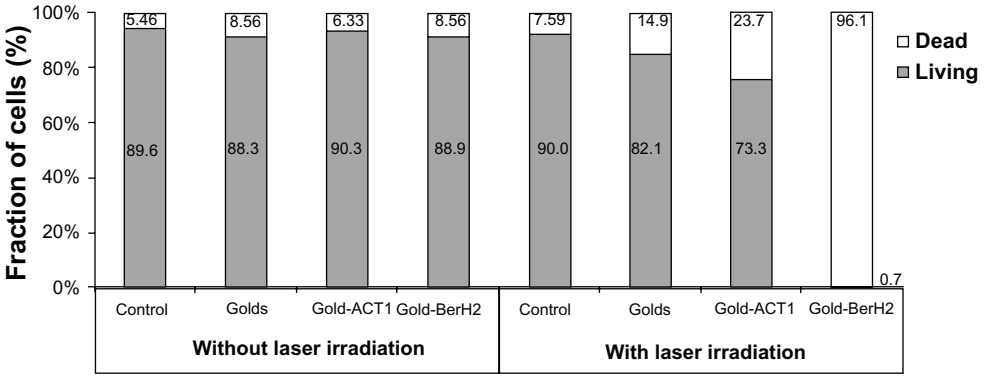

Figure 6 The influence of gold nanoparticles on the viability of L428 cells under four different conjugation conditions: without gold (Control), with unbound golds (Golds), with gold-ACT1 conjugates (Gold-ACT1), and with gold-BerH2 conjugates (Gold-BerH2).
Note: Each test included one group with and one group without laser irradiation.

cell viability between the four cell samples without laser irradiation. The presence of gold did not influence cell viability. In the irradiated part, there was no significant difference from the control group in the cell viability. For the cells in the unbound gold group and in the gold-ACT1 conjugates group, a slight increase in the death rate can be found. Due to the small volume of the sample micro-cuvettes, gold or gold-ACT1 conjugates in the sample volume might distribute in the surrounding cells, which could induce some heat energy shift to the cells. Compared with the other three groups, due to the specific coupling of CD30 antigen and BerH2 antibody, gold-BerH2 conjugates have a tight binding on the surface of L428 cells. Under laser irradiation with 40 mW, 5 pulses, a large damage rate of about 96% was observed in the L-428 cells.

Discussion

With the preliminary successes of photothermal therapy in cancer studies, gold nanoparticle-mediated thermal therapy became a new and minimally invasive tool for cancer treatment.[19,20] In the present study, to evaluate the effectiveness of gold in the destruction of cancer cells or tumor tissue, three main aspects were considered: the photothermal therapy system, specific gold nanoparticle–antibody conjugates, and different experimental parameters. We set up a photothermal therapy system (Figure 1). A pulsed light with 532 nm wavelength was chosen to match the surface plasmon resonance absorption peak of 15 nm gold nanoparticles used in the experiment for photothermal cancer treatment.

Specificity of targeting to achieve high efficiency of photothermal conversion of gold nanoparticles was a key problem. There should be substantial diversity in cellular uptake among the different gold nanoparticle–antibody conjugates and different cell types. Specific targeting should produce a high photothermal effect on the targeted cancer, and only minimal heat should be applied to the surrounding normal cells and tissues. After synthesizing two different gold nanoparticle–antibody conjugates, gold-BerH2 and gold-ACT1 conjugates, their conjugation stability and binding specificity for L-428 cells were evaluated (Figure 2). L-428 cells are positive for CD30, but negative for CD25. Through flow cytometry measurements using Alexa 488, there were obvious differences between these two conjugates targeted cells and fluorescence intensity. The results indicate that the gold-BerH2 conjugates bound specifically to the surface of L-428 cells, but that gold-ACT1 conjugates did not, which seems to agree with our predictions.

Prior to considering gold nanoparticles for photothermal therapy application, it is important to understand their characterization of biocompatibility.[21] The toxicity and side effects of nanoparticles are determined by the shape, dose, surface chemistry, incubation duration, etc.[22–24] We compared the toxicity of pure gold nanoparticles and gold–antibody conjugates to L-428 cells under different incubation time periods and different concentrations. After incubation for 24 hours, pure gold and gold–antibody conjugates incubated with L-428 cells did not induce a decrease in cell viability compared with control cells under a relatively low concentration (the ratio of gold to cells was not more than 10^4:1); but, with an increase in the gold concentration, a decrease in cell viability was observed. A relatively low concentration of gold and a short incubation time were adopted in the photothermal experiment to exclude the influence of cytotoxicity of gold on cell viability.

During the photothermal treatment, the temperature distribution on the surrounding cell surface was the dominant factor leading to cell death.[25–26] It is important to note that the temperature distribution is determined by

the gold's shape and concentration and the wavelength and power of laser irradiation. At the molecular level, hyperthermic effects can induce protein denaturation, membrane rupture, and cell shrinkage.[27] Cytotoxic effects have occurred in cells maintained for 1 hour at 42°C, but this duration could be shortened to 3–4 minutes by using a higher temperature such as 80°C.[14,27–29] Numerical analysis found that cells with higher gold-loading required a lower laser-irradiated power to achieve the temperature rise for cell destruction.[14] Photothermal therapy tests on living L-428 cells were initially performed to confirm the gold nanoparticle-mediated photothermal effect on cell viability. When cells were treated with gold or laser alone, few damaged cells were detected. After laser irradiation in the presence of the gold, the cell death rate had a severe increase (Figure 4), and the results were also confirmed by fluorescence microscopy. With the combination of gold nanoparticles and laser irradiation, few calcein-AM positive cells were observed and most L428 cells were positive for PI staining. The effect of laser irradiation on cell damage has been evaluated (Figure 5). For the control cells without gold, there was no remarkable change in cell viability when increasing the power of laser irradiation. But in the presence of gold-BerH2 conjugates, cell damage efficiency was affected significantly by the laser-irradiated power, and the cell death rate mostly depended on the power of laser irradiation. For successful cancer killing, the cells must be heated to a minimum temperature by proper laser irradiation to cause cancer cell death. The different binding mode of gold to cells can also induce different therapy efficiency on cell viability (Figure 6). Under the same laser irradiation, the specific binding of gold-BerH2 conjugates to L-428 induced extensive cell damage, but there was a slight increase in the cell death rate for the nonspecific binding groups, cells with the unbound gold group, and cells with the gold-ACT1 conjugates group. The results again confirmed the advantage of specific targeting of gold to cells and high therapy efficiency for gold-targeted cancer cells and slight damage to untargeted cells.

In vivo photothermal therapy of gold nanostructures in preclinical and, potentially, clinical use is a crucial direction for our future research. Due to the low absorption by tissues in the 700–850 nm near infrared (NIR) region, gold nanostructure-mediated photothermal therapy is predominantly designed to operate in this window of wavelengths to enhance light penetration capability, and to prevent undesirable damage to healthy tissue. The absorption peak of gold nanorods, nanoshells, and nanocages are all in the NIR region. Some recent studies have focused on in vitro and in vivo photothermal cancer treatments;[30–36] however, the optimization of gold nanoparticle-based therapy techniques to physiological environments needs further study, to determine the clinical success of gold nanostructure-based nanomedicine.[19,37,38]

Conclusion

This study investigated the photothermal therapy of golds on Hodgkin's cells. Many experimental parameters, including the absence of gold or laser irradiation, the laser-irradiated power, and the binding mode of gold to cells, were all tested for their influence on cell viability. When conjugated with BerH2 (anti-CD30 receptor) antibodies, these gold nanoparticles specifically bind L-428 cells that overexpress the CD30 receptor; and, with laser irradiation at suitable wavelength and power, very high effectiveness in killing L-428 cells is achieved. Many optimization problems, including the compatibility of gold nanostructures, the stability of gold–ligand conjugates, and laser irradiation modes, need further modification to make them more suitable for in vivo tumor model studies. Gold nanoparticle-mediated photothermal cancer therapy provides a relatively safe microsurgery system for cancer therapy development.

Acknowledgments

We acknowledge Gereon Huettmann, Ramtin Rahmanzadeh, Barbara Flucke, Margit Kernbach, Bever Marco, and Astrid Rodewald from the Institute of Biomedical Optics, University of Lübeck for their assistance during these experiments. We thank the Research Center Borstel for supplying the L-428 cell line and for their help during the preparation of immunooptical probes. This work is supported by the Program of the National Basic Research and Development Program of China (973) under Grant No 2011CB707702, and the National Natural Science Foundation of China under Grant Nos 81090272, 30900334, 60927011, 61108079, and 61120106013.

Disclosure

The authors report no conflicts of interest in this work.

References

1. Boyle P, Levin B. *World Cancer Report 2008*. Lyon, France: International Agency for Research on Cancer Press; 2008.
2. Sutcliffe SB. Cancer control: life and death in an unequal world. *Curr Oncol*. 2012;19(1):12–15.

3. Wust P, Hildebrandt B, Sreenivasa G, Rau B, Gellermann J, Riess H, et al. Hyperthermia in combined treatment of cancer. *Lancet Oncol*. 2002;3:487–497.
4. El-Sayed IH, Huang X, El-Sayed MA. Surface plasmon resonance scattering and absorption of anti-EGFR antibody conjugated gold nanoparticles in cancer diagnostics: applications in oral cancer. *Nano Lett*. 2005;5(5):829–834.
5. Hirsch LR, Stafford RJ, Bankson JA, et al. Nanoshell-mediated near-infrared thermal therapy of tumors under MR guidance. *Proc Natl Acad Sci U S A*. 2003;100:13549–13554.
6. Voliani V, Ricci F, Signore G, Nifosì R, Luin S, Beltram F. Drug delivery: multiphoton molecular photorelease in click-chemistry-functionalized gold nanoparticles. *Small*. 2011;7(23):3270.
7. Jain PK, El-Sayed IH, El-Sayed MA. Au nanoparticles target cancer. *Nano Today*. 2007;2:16–27.
8. Fernandez Cabada T, de Pablo CS, Serrano AM, Guerrero Fdel P, Olmedo JJ, Gomez MR. Induction of cell death in a glioblastoma line by hyperthermic therapy based on gold nanorods. *Int J Nanomedicine*. 2012;7:1511–1523.
9. Loo C, Lowery A, Halas N, West J, Drezek R. Immunotargeted nanoshells for integrated cancer imaging and therapy. *Nano Lett*. 2005;5(4):709–711.
10. El-Sayed IH, Huang X, El-Sayed MA. Selective laser photo-thermal therapy of epithelial carcinoma using anti- EGFR antibody conjugated gold nanoparticles. *Cancer Lett*. 2006;239:129–135.
11. Pitsillides CM, Joe EK, Wei X, Anderson RR, Lin CP. Selective cell targeting with light-absorbing microparticles and nanoparticles. *Biophys J*. 2003;84(6):4023–4032.
12. Zharov VP, Galitovsky V, Viegas M. Photothermal detection of local thermal effects during selective nanophotothermolysis. *Appl Phys Lett*. 2003;83(24):4897–4899.
13. Zharov VP, Kim JW, Curiel DT, Everts M. Self-assembling nanoclusters in living systems: application for integrated photothermal nanodiagnostics and nanotherapy. *Nanomedicine.* 2005;1(4)326–345.
14. Huang X, Jain PK, El-Sayed IH, El-Sayed MA. Determination of the minimum temperature required for selective photothermal destruction of cancer cells with the use of immunotargeted gold nanoparticles. *Photochem Photobiol*. 2006;82(2):412–417.
15. Huang X, El-Sayed IH, Qian W, El-Sayed MA. Cancer cell imaging and photothermal therapy in the near-infrared region by using gold nanorods. *J Am Chem Soc*. 2006;128(6):2115–2120.
16. O'Neal DP, Hirsch LR, Halas NJ, Payne JD, West JL. Photo-thermal tumor ablation in mice using near infrared-absorbing nanoparticles. *Cancer Lett*. 2004;209(2):171–176.
17. Chen J, Wang D, Xi J, et al. Immuno gold nanocages with tailored optical properties for targeted photothermal destruction of cancer cells. *Nano Lett*. 2007;7(5):1318–1322.
18. Khlebtsov NG, Bogatyrev VA, Melnikov AG, Dykman LA, Khlebtsov BN, Krasnov Ya M. Differential light-scattering spectroscopy: a new approach to studying of colloidal gold nanosensors. *J Quant Spect Radiat Transf*. 2004;89(1–4):133–142.
19. Kennedy LC, Bickford LR, Lewinski NA, et al. A new era for cancer treatment: gold-nanoparticle-mediated thermal therapies. *Small*. 2011;7(2):169–183.
20. Dykman L, Khlebtsov N. Gold nanoparticles in biomedical applications: recent advances and perspectives. *Chem Soc Rev*. 2012;41:2256–2282.
21. Krishnan S, Diagaradjane P, Cho SH. Nanoparticle-mediated thermal therapy: evolving strategies for prostate cancer therapy. *Int J Hyperthermia*. 2010;26:775–789.
22. Murphy CJ, Gole AM, Stone JW, et al. Gold nanoparticles in biology: beyond toxicity to cellular imaging. *Acc Chem Res*. 2008;41(12):1721–1730.
23. Lewinski N, Colvin V, Drezek R. Cytotoxicity of nanoparticles. *Small*. 2008;4(1):26–49.
24. Chen J, Glaus C, Laforest R, et al. Gold nanocages as photothermal transducers for cancer treatment. *Small*. 2010;6(7):811–817.
25. Noguez C. Surface plasmons on metal nanoparticles: the influence of shape and physical environment. *J Phys Chem C*. 2007;111(10):3806–3819.
26. Harris N, Ford MJ, Cortie MB. Optimization of plasmonic heating by gold nanospheres and nanoshells. *J Phys Chem B*. 2006;110(2):10701–10707.
27. Habash RW, Bansal R, Krewski D, Alhafid HT. Thermal therapy, part 1: an introduction to thermal therapy. *Crit Rev Biomed Eng*. 2006;34(6):459–489.
28. Hildebrandt B, Wust P, Ahlers O, et al. The cellular and molecular basis of hyperthermia. *Crit Rev Oncol Hematol*. 2002;43:33–56.
29. Dewey WC. Arrhenius relationships from the molecule and cell to the clinic. *Int J Hyperthermia*. 1994;10:457–483.
30. Liu Y, Wang H. Nanomedicine: nanotechnology tackles tumours. *Nat Nanotechnol*. 2007;2(1):20–21.
31. Zhang Q, Xie J, Lee JY, Zhang J, Boothroyd C. Synthesis of Ag@AgAu metal core/alloy shell bimetallic nanoparticles with tunable shell compositions by a galvanic replacement reaction. *Small*. 2008;4:1067–1071.
32. Tong L, Zhao Y, Huff TB, Hansen MN, Wei A, Cheng JX. Gold nanorods mediate tumor cell death by compromising membrane integrity. *Adv Mater*. 2007;19:3136–3141.
33. von Maltzahn G, Park JH, Agrawal A, et al. Computationally guided photothermal tumor therapy using long circulating gold nanorods antennas. *Cancer Res*. 2009;69:3892–3900.
34. Gobin AM, Watkins EM, Quevedo E, Colvin VL, West JL. Near-infrared-resonant gold/gold sulfide nanoparticles as a photothermal cancer therapeutic agent. *Small*. 2010;6(6):745–752.
35. Chen J, Glaus C, Laforest R, et al. Gold nanocages as photothermal transducers for cancer treatment. *Small*. 2010;6(7):811–817.
36. Samim M, Prashant CK, Dinda AK, Maitra AN, Arora I. Synthesis and characterization of gold nanorods and their application for photothermal cell damage. *Int J Nanomedicine*. 2011;6:1825–1831.
37. Cai WB, Gao T, Hong H, Sun J. Applications of gold nanoparticles in cancer nanotechnology. *Nanotechnol Sci Appl*. 2008;1:17–32.
38. Arvizo RR, Bhattacharyya S, Kudgus RA, Giri K, Bhattacharya R, Mukherjee P. Intrinsic therapeutic applications of noble metal nanoparticles: past, present and future. *Chem Soc Rev*. 2012;41:2943–2970.